HHS Public Access

Author manuscript

Cell Rep. Author manuscript; available in PMC 2022 May 06.

Published in final edited form as:

Cell Rep. 2022 April 12; 39(2): 110651. doi:10.1016/j.celrep.2022.110651.

Uptake, functionality, and re-release of extracellular vesicle-encapsulated cargo

Killian O'Brien[1,2,*], **Stefano Ughetto**[3], **Shadi Mahjoum**[1,2], **Anil V. Nair**[4], **Xandra O. Breakefield**[1,2,5,*]

[1]Molecular Neurogenetics Unit, Department of Neurology and Center for Molecular Imaging Research, Massachusetts General Hospital and Harvard Medical School, Boston, MA, USA

[2]Department of Radiology, Massachusetts General Hospital and Harvard Medical School, Boston, MA, USA

[3]Department of Oncology, University of Turin, 10060 Candiolo, TO, Italy

[4]Program in Membrane Biology, Division of Nephrology, Massachusetts General Hospital and Harvard Medical School, Boston, MA, USA

[5]Lead contact

SUMMARY

Extracellular vesicles (EVs) are membrane-encapsulated particles that carry genetically active and protein/lipid cargo that can affect the function of the recipient cell. A number of studies have described the effect of these vesicles on recipient cells and demonstrated their promise as therapeutic delivery vectors. Here we demonstrate functional delivery of EV-encapsulated RNA and protein cargo through use of luminescence and fluorescence reporters by combining organelle-targeted nanoluciferase with fluorescent proteins. We highlight a mechanism by which cells retain internalized cargo in the endosomal compartment for days, usually leading to content degradation. We also identify a mode through which recipient cells re-release internalized EVs intact after uptake. Highlighting these different fates of EVs in recipient cells sheds light on critical factors in steering functional cargo delivery and will ultimately allow more efficient use of EVs for therapeutic purposes.

Graphical Abstract

*Correspondence: killianpob@gmail.com (K.O.), breakefield@hms.harvard.edu (X.O.B.).

AUTHOR CONTRIBUTIONS

K.O. designed and performed experiments and wrote the manuscript. S.U. designed and performed experiments. S.M. performed experiments. A.V.N. performed imaging. X.O.B. designed experiments and secured funding. All authors edited the manuscript.

DECLARATION OF INTERESTS

The authors declare no competing interests.

SUPPLEMENTAL INFORMATION

Supplemental information can be found online at https://doi.org/10.1016/j.celrep.2022.110651.

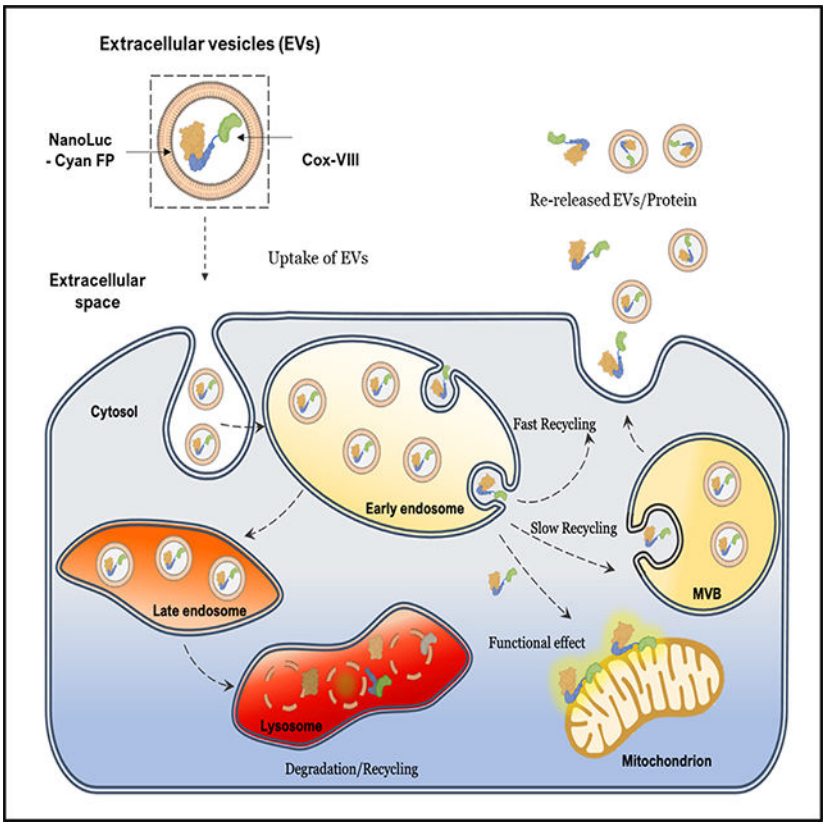

In brief

O'Brien et al. demonstrate functional and non-functional internalization of EV cargo and re-release of previously internalized particles. This highlights another obstacle for functional delivery of EV-internalized cargo for therapeutic purposes.

INTRODUCTION

Extracellular vesicles (EVs) were initially envisioned as garbage disposal units for cells (Pan and Johnstone, 1983) but have since also been reported to contain and transfer genetic material and other informational cargo in a functional manner between cells (Ratajczak et al., 2006; Valadi et al., 2007; Skog et al., 2008). Since this realization, much work has been invested in elucidating the biogenesis, secretion, distribution, content, and functionality of EVs. This paper focuses on the functionality and fate of EVs after uptake into recipient cells. There are many routes by which EVs can enter a recipient cell—macropinocytosis, lipid-raft-mediated uptake, phagocytosis, and membrane fusion (Mulcahy et al., 2014; Mathieu et al., 2019)—with some reports of tunneling nanotubes mediating transfer (Rustom et al., 2004). Based on published literature, it appears that the main route of EV uptake is via clathrin/caveolin-mediated endocytosis (Mulcahy et al., 2014). For functional delivery, EV-encapsulated content must then "escape" the endosome into the cytoplasm prior to progressive acidification of this organelle, which results in eventual degradation of the cargo (Iversen et al., 2011). Escaping from the endosomal pathway is then a necessary process for

functional delivery (Hung and Leonard, 2016). Viruses (Schnell and Chou, 2008; Grove and Marsh, 2011) and bacteria (Geoffroy et al., 1987; Tweten, 2005) have developed specialized mechanisms through which they exploit the low-pH environment of the endosome to escape into the cytoplasm. Whether EVs have developed similar or unique mechanisms remains unknown. Because of this obstacle, it is critical to robustly demonstrate functional delivery of EV-encapsulated content to recipient cells to support their communicative properties.

Endosomal escape and functional delivery of cargo are desired outcomes for therapeutic use of EVs, but there is also the potential for loss of cargo because of degradation, recycling in the cell (repurposing) of cargo, or re-release of intact vesicles into the extracellular space. All of these processes abort functional transfer of EV cargo into the recipient cell. Fast and slow recycling endosomes exist in the overall endocytosis pathway (Hopkins, 1983; Hopkins and Trowbridge, 1983), and these processes have been relatively well characterized (Cullen and Steinberg, 2018). Since 1983, receptor-mediated uptake and re-release of the transferrin receptor has been determined (Harding et al., 1983), but whether a parallel process exists for EV cargo is unclear. EV uptake and recycling would not be novel mechanisms because re-use of components has been identified from redistribution of lipids and repurposing of membrane proteins to functionally assist with drug resistance (Tian et al., 2010; Wang et al., 2019). Retention and recycling of internalized cargo have been described since 1995 (Marsh et al., 1995), so there is the possibility that this may exist as a "normal" route after EV uptake. There is a better-studied relationship between viruses and the recycling endosome, where the compartment can facilitate functional uptake in the case of the vaccinia virus (Hsiao et al., 2015) but can also result in recycling of material to the plasma membrane (Zila et al., 2014). Rab11, associated with the recycling endosome, can play a role in the more commonly studied trafficking and exocytosis of viruses such as influenza A virus (Momose et al., 2011), hantavirus (Rowe et al., 2008), and respiratory syncytial virus (Utley et al., 2008). Identifying a process resulting in re-release of EVs and their content may elucidate another avenue resulting in non-functional delivery. The potential process of EV recycling or re-release has been suggested by others (Mathieu et al., 2019). There remains a need for definitive data to demonstrate whether these processes occur for intact EVs and their content.

This paper reports our efforts to robustly demonstrate functional uptake of specific EV-encapsulated mRNA and protein. It was necessary to use exceptionally sensitive and versatile tools. Nanoluciferase (Nluc) (Hall et al., 2012) is an extremely bright and small (19.1-kDa) bioluminescent protein, allowing it to be easily quantified and even fused to other proteins. Suzuki et al. (2016) created constructs through fusion of Nluc to coxVIII (Cox), H2B, and myristoylation/palmitoylation (Lyn), which were fused to cyan, red, and orange fluorescent proteins, respectively. The Cox construct localizes a fluorescent signal to the mitochondrial membrane, increasing the potential of visualizing cytoplasmic uptake of EV content. The H2B construct focuses expression of the protein to the nucleus, which restricts EV release of the protein, and the Lyn construct is useful for tracking the fate of EV membranes. Such tools allows sensitive quantitation of the luminescent signal and visualization of the fluorescent signal in a cellular compartment. Coupling luminescent and fluorescent readouts should help to elucidate the fate and functions of EV cargo. Although functionality of EV cargo is the desired output, this study also sought to evaluate

the possible re-release of EVs with their content intact. Using these tools facilitated identification of such processes.

This paper validates the capacity for EVs to deliver cargo functionally to a recipient cell and highlights the relative inefficiency, at least in the tested cells. It also highlights a fate resulting in cargo retention in the endosomal pathway with eventual rerelease from the same cell. This retention and re-release of delivered EVs is another barrier to obtaining functionally efficient EVs.

RESULTS

Before we could track the fate of EV cargo in recipient cells, it was necessary to first demonstrate that EVs are, in fact, being isolated and that the protein of interest is encapsulated within the vesicles. Conditioned medium from HEK293T (HEK) cells transfected with an expression plasmid for Cox (Suzuki et al., 2016) was concentrated using UFC9100 Amicon Ultra-15 centrifugal filters (100 kDa), and EVs were separated by size-exclusion chromatography (SEC) (Guerreiro et al., 2018). For this project, the protein was loaded into vesicles based on overexpression of the construct in the donor cell (Haney et al., 2013; Wiklander et al., 2019). Although most of the overexpressed bioluminescent Cox was released as protein into the medium in fractions 12–30 (Figure S1A), fractions 7–11 were designated as containing EVs based on being the first peak evident, as described previously (Benedikter et al., 2017; Pedersen et al., 2013). Isolated EVs were further concentrated by filtration (30 kDa). To ensure that EVs were not damaged by the sheer force exerted upon them by centrifugation filtration, samples were run through SEC again (Figure 1A). These data show purification of the EV population and removal of the latter protein fractions. To demonstrate that this signal was in EVs, fractions 7–11 were incubated with Proteinase K to determine whether the protein was protected by a membrane; a protein fraction was also included to demonstrate the efficacy of Proteinase K (Figure 1B). Although there was a significant reduction in signal from protein fraction 19 incubated with the enzyme, there was no difference in signal between treated and non-treated conditions of EVs. This demonstrated that the EV membrane protected the cargo protein from degradation and that there was not a detectable level of non-encapsulated protein in collected fractions 7–11. It was possible to release this encapsulated signal when EVs were treated with 1% Triton X-100, which permeabilizes the protective membrane, exposing the protein to the enzyme Proteinase K (Figure 1C).

Protein incubation with Triton X-100 also confirmed that the detergent affected neither the Cox substrate furimazine or the enzyme Proteinase K (Figure S1B). To characterize EVs with typical markers, samples were incubated with CD63 and CD9 immunoaffinity beads (Pedersen et al., 2013; Oksvold et al., 2015) to determine whether there was binding of the signal to the beads. From the entire sample of isolated EVs, there was detectable signal associated with CD9 (64.1%; Figure 1D) and CD63 (17.2%; Figure S1C), whereas incubation of beads with protein fractions resulted in 1.1% and 1.4% retention, respectively (Figures S1D and S1E). To demonstrate that signal associated with CD9 and CD63 beads contained encapsulated proteins, samples were incubated with Triton X-100 and beads were separated from the supernatant. This resulted in a reduction in CD9/63 bead-associated

signal compared with the control (PBS) and an increase in signal present in the supernatant (Figures 1E and S1F), confirming that the luminescent signal was in the EVs.

HEK cells were used as donor cells because they are relatively easy to transfect with DNA at high efficiency. HeLa cells were used as recipients because they have been reported to be effective recipient cells for EV transfer from a variety of cells (Svensson et al., 2013; Costa Verdera et al., 2017). Knowing that the reporter and other proteins were in EVs, the next step was to evaluate uptake of the EVs into recipient HeLa cells. EVs were isolated by SEC and filtration from HEK cells and added to recipient HeLa cells, and uptake was measured by bioluminescence of recipient cells. To ensure that the delivered protein was internalized into the recipient cells, they were treated with 0.25% trypsin-EDTA for 30 min at 37°C to remove any non-internalized EVs (Xiao et al., 2008; Ali et al., 2016) from the cell surface and then washed and pelleted by centrifugation (2,000 × *g* for 5 min) in 1× PBS twice. Recipient cells were incubated with EVs for 72 h, and during that time, there was a continuous increase in internalization (Figure 2A). This suggests that, when EVs are in excess, cells will continually internalize the vesicles, with the apparent increase resulting from increased recipient cell numbers through proliferation (Figure S2A). Comparing the efficiency of EVs with protein alone, uptake of EVs was significantly more efficient than free protein after 24 h (Figure 2B). However, the uptake efficiency of EV cargo remained below 1%.

Because protein content is evidently in EVs and internalized by the recipient cells, the next step was to assess the presence and functionality of mRNA delivered by EVs. For this, the H2B construct was used because the protein expressed is preferentially incorporated into the nucleus and would therefore be less likely to be packaged into EVs at a rate equivalent to a cytosolic protein. This mRNA is 2.2 kb, a size that should not restrict its incorporation into EVs (Wei et al., 2017). The assay design is outlined in Figure 2C; a population of EVs does not carry detectable levels of the H2B protein but mRNA compared with EVs isolated from another population of cells that carry mRNA and H2B protein, based on the length of time after transfection with an expression plasmid. Primers specific to this construct were designed, and the 5′ section and 3′ section were detected in EVs by qPCR (Figure 2D). The 3′ fragment was expressed at higher levels compared with the 5′ fragment, mirroring previous findings (Wei et al., 2017). *HPRT1* was used as a housekeeping gene to normalize for equivalent sample loading. To evaluate the functionality of the H2B mRNA, EVs were isolated from non-transfected cells (control) and from cells transfected with the H2B expression plasmid for 6 h and 24 h. The protein was not detectable in the 6-h EVs by bioluminescence, whereas it was robustly present in the 24-h EVs (Figure 2E). Twenty-four hours after transfer to cells treated with cycloheximide to block new protein synthesis or left untreated, there was a significant increase in signal from cells exposed to 6-h EVs in non-treated versus treated cells after 6 h (Figure 2F), whereas there was no significant change evident in the conditioned medium of the same treated cells from time (T)0 to T24 (Figures S2B and S2C). It was also important to show that cycloheximide-treated cells could still internalize EVs, as shown in Figure S2D. To ensure that the observed effects were not derived from transfer of the expression construct (plasmid DNA) in the transfection medium, the experiment was repeated in the absence of donor cells to show that the results were not derived from transfection of recipient cells (Figures S2E and S2F).

Functional delivery of the mRNA for the H2B construct was evident, but we also wanted to show delivery of protein to recipient cells by its localization in a specific organelle. Cox has a mitochondrial localization signal whereby fluorescent imaging could determine whether the protein in the EVs entered the cytoplasm and moved to the mitochondria. To evaluate this, HeLa cells stably expressing palmTdTomato, which labels all cell membranes (Lai et al., 2014), were incubated with HEK-derived Cox EVs and imaged by confocal microscopy (Figures 3A, 3B, S3A, S3B, S3D, and S3E). When the fluorescence profile of Cox and a mitochondria label (Tom20) were analyzed, there was clearly a similar intensity profile (Figures 3C, S3C, and S3F). These images point to the capacity of Cox to enter the recipient cells via EVs and associate with the mitochondrial membrane. Although this may not be evident for every delivered protein, the capacity for exit from the endosome was clearly evident here. To analyze functional delivery, a cell fractionation assay was performed on HeLa cells that were incubated with Cox EVs (Figure 3D). These results showed robust signal in the cytosol and mitochondrial fractions. It was also important to determine whether the relatively low signal detected in each cellular fraction was a consequence of signal saturation for the cell or whether it was the limit of cell internalization. A "standard curve" of EVs was added to recipient cells, and the cell fractionation assay was performed (Figures 3E and 3F). Although there was a significant reduction in EV signal in the medium, there was no significant difference in the percentage of uptake between the 100% and 50% groups, whereas there was no detectable uptake in the 25% group.

It appeared that some proteins were delivered in an active state by EVs; it was also clear that another subset of the internalized protein appeared to be retained in apparent endosomal compartments. Because palmitoylated proteins label cell membranes (McCabe and Berthiaume, 1999), they can be used as a surrogate for endosomal membranes. To examine this, the same images as shown in Figure 3 were analyzed to evaluate whether the Cox protein signal also appeared to align, in certain cases, with internal palmitoylated membranes (Figures 4A, 4B, S4A, S4B, S4D, and S4E). In this case, these images were captured after incubation of the cells in Cox EV-free medium for 24 h. Therefore, these cells had not internalized the EVs within the last 24 h. The fluorescence intensity profile showed co-localization of the EV and palmitoylated membrane profile, whereas there was no co-localization with the mitochondrial marker (Tom20) (Figures 4C, S4C, and S4F). To examine this, cell fractionation was again performed on cells that had external Cox-EVs removed for 24 h prior to analysis (Figure 4D). There was localization of signal between the palmTdTomato and the Cox protein, suggestive of localization of the Cox protein in the endosomal compartment. Because this signal did not localize with the mitochondria, it is suggestive of retention in the membrane dense endosome. This signal had not internalized within the previous 24 h and was therefore being retained in the cell in a "non-functional" manner. Next we used the Lyn construct, which is attached to the membrane of the vesicles, and saw retention of this signal in the cells 24 h after removal of external EVs, suggesting retention in EVs (Figure 4E). Although it may be possible that this signal is derived after fusion of the EVs to the membrane of the cell or endosome, we do not believe this to have occurred at such a rate that it would be detectable by our methods. Because the reporter was tagged to the membrane of the vesicles and should not be targeted to any other locations in

the recipient cell, detection of the protein in discrete structures suggests that vesicles were retained in endosomes.

Because it seemed that some EVs were retained in the endosomes for a period of time after uptake and others released functional cargo into the cytoplasm, we also analyzed the possibility that the same EVs may be re-released intact from the cells. We added EVs from cells transfected with Lyn to label the membranes of the vesicles. The EVs with labeled membranes were incubated with the recipient cells for 48 h, the surface of these cells was washed extensively by low-level trypsinization, and then cells were re-seeded in fresh medium devoid of any Lyn EVs (Figure 5A). The purpose of this was to detect any signal in the medium after incubation of the re-seeded cells. Any signal in the medium must originate from the cells that had initially internalized the vesicles. There was a clear signal detected in the medium of the cells previously exposed to EVs after 24 h that was not present at 0 h (Figure 5B). Concurrent with the increased signal in the medium, there was a decreased signal in the cells (Figure 5C). To show that a portion of the re-released signal was in vesicles, the medium was run through SEC, and the EV fractions (7–11) were analyzed, revealing an increase in signal in the Lyn EV population versus the control (Figure 5D).

Although the Lyn construct was useful to track the fate of lipid membranes, it would also be important to see whether EV-encapsulated cargo could also be re-released. This experiment was designed similarly as that in Figure 5 but used EVs derived from cells transfected with Cox (Figure 6A). When analyzing conditioned medium, signal was detected 24 h after re-seeding, whereas there was no signal evident in the conditioned medium at 0 h (Figure 6B). To show that the Cox protein is primarily retained within the cell membrane, cells were transfected with the Cox construct for 3 h, resulting in robust signal in the cells that was not detected in the medium. This demonstrates that the protein, when not overexpressed, remains in the cells, highlighting a unique mode of re-release in the cells that were exposed to EVs (Figure S5A). Although the signal appeared to increase in the medium, there was a decline of signal in the cells at 24 h (Figure 6C). When incubating at each time point with CD9 beads, the signal was also detected, suggesting encapsulation of a portion of the signal in $CD9^+$ EVs (Figure 6D), whereas there was still signal in the $CD9^-$ medium (Figure S5B). To ensure that the transfection reagent was not a source of this signal, a sample without cells but with transfection reagent was treated as EVs and transferred to recipient cells but did not produce any signal (Figure S5C). To remove an increase in cell death as a source of re-release, an LDH (lactate dehydrogenase) assay was performed to show that experimental handling did not increase cell death (Figures S5D and S5E). This, coupled with the data from Lyn EVs, supports re-release of some EVs intact after cellular internalization.

DISCUSSION

This paper assesses and demonstrates functional delivery of proteins and mRNAs by EVs, as indicated by previous studies. In addition, we also demonstrate a process by which cells can re-release EVs and their content after cellular internalization. These studies support use of EVs as delivery vehicles, but with caveats regarding efficiency of functional delivery, at least with respect to the EV source and tested recipient cells.

When analyzing events that occur at a nanoscale level, such as EV fate, it is important to have the appropriate tools for analysis. In this study, we adapted the use of reporter constructs that have fluorescence and luminescence signals and also localize to specific organelles in cells (Suzuki et al., 2016). Nluc is a highly sensitive luminescent protein and allows robust detection in nanoparticles, EVs, and cells (Hall et al., 2012). Focused fluorescence in subcellular locations can facilitate visualization of the fluorescent protein after entry into or translation in the recipient cell cytoplasm. Delivery of a non-localized fluorescent protein via EVs is more difficult to assess because, when it leaves the endosome, the signal is diluted in the recipient cell cytoplasm (Selby et al., 2017), so adding a localization signal serves to concentrate the signal in a specific subcellular region. When evaluating mechanisms of action of EVs taken up by cells, it is critical to isolate a pure population of vesicles with minimal damage to these nanoparticles. Although there are many suggested methods of isolating EVs (Théry et al., 2018), there are positives and negatives to each technique. For this study, SEC was used exclusively for the purpose of separating "contaminating" non-encapsulated proteins from EVs (Benedikter et al., 2017), and the enriched EV fraction was used "fresh" (i.e., immediately after collection with no freezing). With the mitochondrially localized Nluc Cox, we showed that the fractions (7–11) we identified as EVs contained a high amount of membrane-protected (EV encapsulated) protein and non-detectable levels of free (non-encapsulated) protein. In this study, although non-encapsulated protein does not enter recipient cells as efficiently as EV-encapsulated protein, it can still be responsible for some signal seen in the EV preparation and subsequent transfer studies (Ludwig et al., 2019). Handling techniques to isolate EVs often involve centrifugation, whether for separation or concentration (Benedikter et al., 2017). Such force on EVs can affect the collected isolates (Linares et al., 2015) and may affect the integrity of the membrane, resulting in free protein in the preparation. In this study, we elucidate a method by which the force exerted on the EVs by Amicon filter concentration does not detectably introduce free protein into the final EV preparation. Although this method may not be relevant for all studies related to EVs, it can at least isolate a population of highly pure EVs that maintain functionality in an *in vitro* context.

Although functional delivery of cargo via EVs has been reported for some time (Ratajczak et al., 2006; Valadi et al., 2007; Skog et al., 2008), there is still a deficiency in robust and quantitative demonstration of specific functional uptake of EV-encapsulated content. As of now, the most prevalent mechanism of uptake for EVs appears to be via endocytosis; thus, it would make sense for EVs to have a mechanism for releasing their cargo into the cytosol. Some studies suggest that EVs can escape the endosome/lysosome via fusion/permeabilization (Joshi et al., 2020; Polanco et al., 2021). At this point, we can assume that it is likely to occur by several different mechanisms. Uptake of EV content without functional analysis of cargo can simply refer to cellular internalization of cargo. Because endocytosis is a commonly projected route of EV entry (Mathieu et al., 2019), uptake does not equate to functionality because contents may be degraded through maturation of endosomes to lysosomes. In this study, we initially demonstrated uptake/internalization of EV-encapsulated proteins, but this is not sufficient to conclude that the content is functional or has even entered the cytoplasm of the recipient cell. Although certain EVs may have a functional effect on the recipient cell without entry into the cytoplasm (e.g.,

activation of T cell receptors; Raposo et al., 1996; Tkach et al., 2017; O'Brien et al., 2020), most therapeutic uses for EVs require delivery of encapsulated content into the cytoplasm (Gurunathan et al., 2019). In this study, using a dual reporter Cox protein (Suzuki et al., 2016), we showed, through fluorescence, that the encapsulated protein enters the cytoplasm of the recipient cell and localizes to the mitochondrial membrane. There is evidence suggesting that mitochondria may be transferred via EVs, and this may be a factor in this study, but the overwhelming majority of the protein in this study appears not to be associated with mitochondria because it is present in EVs and as free protein whereas mitochondria generally are not (Qin et al., 2021). We confirmed functional uptake by luminescence, highlighting the benefit of such a powerful reporter. This demonstration of EV cargo delivery to the cell cytoplasm confirms that EVs have the capacity to deliver their cargo to recipient cell cytoplasm, but we found this process to be inefficient with the donor (HEK) and recipient (HeLa) cells we used.

When proving functional delivery of cargo, it became evident that some cargo was retained in what appeared to be the endosomal compartment. Using the same strategies as for functional delivery, we showed that some of the EVs remain within the cell in a "non-functional" manner. Using the Nluc Lyn membrane construct (Suzuki et al., 2016), we showed that a portion (roughly 17%) of the overall internalized signal is retained in the cell 24 h after removing the external source of the signal. Combining these results suggests a possible mechanism of retaining cargo in endosomes of the cell prior to degradation or possible rerelease. The determining factor for this fate remains unclear, but it will be important to elucidate this to improve the efficiency of EV-delivered cargo.

Endocytosis has been highlighted as a bottleneck for functional delivery (Hung and Leonard, 2016), but there may be other compounding factors that can affect the efficacy of EV delivery. The recycling endosome is a potential route (Cullen and Steinberg, 2018) that acts to release proteins and lipids that have entered via endocytosis and redistributes them to the plasma membrane with subsequent exocytosis (van Ijzendoorn, 2006). The Lyn construct allowed tracking of membrane-associated EV lipids after internalization. Here we saw this protein re-released into the medium from cells after uptake and, more importantly, could detect it in released EVs. These results are suggestive of a mechanism whereby EVs can enter a cell and subsequently be re-released intact from the same cell.

To build on this, it was important to evaluate whether EVs that carry proteins with a cell organelle localization signal may subsequently be re-released with the protein contained in the EVs. We demonstrated that this occurs at a detectable level, where the re-released protein is readily detected in the conditioned medium 24 h after thorough trypsinization (0.25% trypsin for 30 min), which would remove all non-internalized EVs, leaving cells intact. This re-released protein was shown to be present in $CD9^+$ vesicles. This provides strong support for the theory that the cargo in the EVs stayed in the vesicle during endocytosis and was ultimately re-released in the same EVs by the cell.

Viruses have been shown to localize to the recycling endosomes upon entry and may be re-released after receptor-mediated endocytosis (Grove and Marsh, 2011; Mainou and Dermody, 2012; Zila et al., 2014). It makes sense that EVs may undergo similar trafficking.

Such a mechanism has not been elucidated previously in relation to EV uptake and internalization. The presence of such a process would suggest that some EVs are sorted into different endosomal pathways, possibly based on the surface components of the vesicles. Surface expression of proteins on an EV dictating its fate is not a novel discovery (Shukla et al., 1999; Christianson et al., 2013; Antes et al., 2018; Hurwitz and Meckes, 2019), but whether certain EVs are re-released because of this surface configuration is another important aspect to consider. This may represent a response from a cell in an environment exposed to an excess of EVs or EVs from a particular cell type and provide a mechanism to prevent unwanted stress on the cell. Although functional delivery of EV content is often the desired outcome, there is an acceptance that endosomal uptake often results in lysosomal degradation with the purpose of recycling or eliminating molecules from the recipient cell (Tian et al., 2010). Bacterial and viral proteins have evolved to adapt to the low-pH environment in the endosomal pathway as a method of delivering cargo into the cytoplasm (Geoffroy et al., 1987; Tweten, 2005; Schnell and Chou, 2008; Grove and Marsh, 2011). Although EVs may have similar mechanisms to deliver content, if there is potential for re-release of content, then this would negate any such adaptive mechanisms. It will be important to better understand how EVs are selected to be re-released so that it can be avoided when using the vesicles for therapeutic delivery.

It is critical to understand all potential fates of EVs in a recipient cell before unleashing the full therapeutic potential of these biologically membrane-enclosed nanoparticles. Although re-release of delivered cargo may not be a desired discovery in relation to functionality of EVs, it is nevertheless an important one to consider. Before designing EVs as efficient delivery tools, it is imperative to fully understand how the vesicles can behave in a recipient cell.

This paper shows that EVs can deliver a protein to the cytosol that subsequently localizes to the mitochondria and that RNA cargo can be translated, although the mechanism of release from the endosome is not fully understood. Re-release of internalized vesicles is just another barrier to functional delivery of EV content. It is accepted that EV cargo reflects, for the most part, the composition of the cell of origin (Valadi et al., 2007; Skog et al., 2008; Hessvik et al., 2012), but the capacity of a cell to re-release internalized cargo suggests that some portion of EVs released from a cell may have been internalized from another source cell. Whether this can occur at a rate to contaminate the overall pool of secreted EVs is not yet clear. It will be important to elucidate the specific factors that regulate functional uptake, cargo degradation, or re-release. Whether these fates are determined by the EV surface components, cell type of the EV source, and/or the recipient cells is not yet clear. All of this new information opens up other avenues of research for determining mechanisms of EV cargo fate after cellular internalization.

Limitations of the study

By addressing functional delivery, this paper defines functionality as localization of the delivered protein to the mitochondria in recipient cell. Although this may not be considered functional because the reporter proteins are not exerting a specific effect, for the purpose of this study, the presence of these proteins in the recipient cell outside of the endosomal

compartments is sufficient. The work in this paper suggests the possibility of cells retaining internalized cargo in a "non-functional" format. Microscopy beyond the scope of this paper could help to shed further light on the specific localization of the cargo and the duration for which it can be retained. This study also highlights the possibility of a mechanism whereby cells re-release previously internalized EVs and their cargo. The exact mechanism has not been outlined in this study and would certainly be worthy of further investigation.

STAR★METHODS

Detailed methods are provided in the online version of this paper and include the following:

RESOURCE AVAILABILITY

Lead contact—Further information and requests for resources and reagents should be directed to and will be fulfilled by the lead contact, Xandra Breakefield (breakefield@hms.harvard.edu).

Materials availability—This study did not generate new unique reagents.

Data and code availability—All data generated and analyzed in this study are available from the corresponding author on reasonable request.

This paper does not report original code.

Any additional information required to reanalyze the data reported in this paper is available from the lead contact upon request.

EXPERIMENTAL MODEL AND SUBJECT DETAILS

Cell lines

Human embryonic kidney 293 (HEK293T) and HeLa cells: Cells were obtained from American Type Culture Collection (ATCC; Manassas, VA, USA) were cultured at 37°C in a 5% CO2 humidified incubator. Culture media was Dulbecco's modified essential medium (Corning) with L-glutamine (Corning) supplemented with penicillin (100 units/mL), streptomycin (100 mg/mL) (P/S) (Corning) and 10% fetal bovine serum (Atlanta Biologics). To generate stable fluorescent cell reporters for confocal-imaging, cells were stably transduced with an expression cassette for a palmitoylation signal (McCabe and Berthiaume, 1999) genetically fused in-frame to the N terminus of tdTomato (PalmtdTom) (Lai et al., 2015) using a CSCW2 lentiviral vector (Sena-Esteves et al., 2004). Cells were routinely tested for mycoplasma contamination (Mycoplasma PCR Detection Kit, abm G238) and found negative.

METHOD DETAILS

Plasmids—pcDNA3-CoxVIIIx2-eNano-lantern (Cox) and Lyn_OeNL_pcDNA3 (Lyn) plasmids were kindly donated by Prof. Nagai, Osaka University (Suzuki et al., 2016) ReNL-H2B_pcDNA3 (H2B) was purchased from Addgene, also originally generated by Prof. Nagai (Suzuki et al., 2016) (Addgene plasmid #89534). All plasmids were transformed into

OneShot™TOP10 Chemically Competent *E.coli* (Thermofisher) with DNA purified using Qiagen Plasmid Maxi kit. All next generation sequencing (NGS) analyses were performed by the CCIB DNA Core Facility at Massachusetts General Hospital (Boston, MA).

Transfection—The plasmids were introduced into HEK293T cells by transfection with polyethylenimine (PEI) (Polyscience, Warrington, PA USA). DNA (2.5 μg) and PEI (1 μg/mL) were mixed to a final volume of 250 μL Opti-MEM® (ThermoFIsher) for 5 min at RT before being combined (500 μL) and let stand at RT for 20 min. This transfection reagent was then added to the cells dropwise and incubated for 18 h.

EV isolation—EVs were isolated by size exclusion chromatography (SEC) using Izon qEVoriginal/70 nm columns as follows. Conditioned media was collected from HEK293T cells seeded in two 150 mm dishes (seeding density ≈2.5×10^6 cells) grown *in vitro* for 48 h and concentrated using UFC9100 Amicon® Ultra-15 Centrifugal filters (100 kDa) centrifuged at 6,000 × g for 10 min at 4°C until all media was concentrated. The concentrated sample (500 μL) was added to the Izon column after washing it with 10 mL 1X phosphate buffer saline, pH 7.4 (PBS; Boston Bioproducts). Then 15 mL PBS was added, and 30 × 0.5 mL fractions were collected using an Izon automatic fraction collector (AFC). Fractions 7 to 30 were collected for full profile analysis. For transfer of EVs, fractions 7–11 were concentrated using Amicon®Ultra-0.5 Centrifugal (30 kDa) to reduce the volume from 2.5 mL to 30–80 μL. For all functional analysis of EVs each step was performed in a sterile manner (i.e. in fume hoods with UV irradiated filters). All functional experiments were conducted using fresh EVs/protein samples and prior to RNA analysis EVs were stored at 4°C for no longer than 72 h.

Luminescent assays—NanoLuc luciferase (Nluc) expression was analyzed with the addition of furimazine (Nano-Glo® Luciferase, Promega) diluted 1 in 500 in 1X PBS. Samples were incubated with the reagent for at least 3 min prior to reading on the BioTek luminometer (Synergy H1 Hybrid Multi-Mode Reader). For readings, samples were either loaded onto translucent 96-well culture plates or 96-well white bottom Greiner Bio-one plates.

EVs/protein analysis—EVs and protein samples, after collection and concentration in PBS, were treated with: Triton X-100 (US Biologicals) made to a working concentration of 1% in PBS and incubated with samples for 30 min with gentle agitation on a HulaMixer™ Sample Mixer (Thermofisher) at RT. Proteinase K (Qiagen) treatment was performed at a final concentration of 100 μg/mL at 56°C for 8 min. For RNaseA treatment of EVs, 1% Triton X-100 was added and incubated for 30 min at RT. RNaseA (Applied Biosystems) was added at a final concentration of 4 U/μL and incubated with EVs at 37°C for 30 min.

CD63/CD9 bead incubation—Ten μl of Exosome – Human CD63 Isolation/Detection (Invitrogen) or Exosome – Human CD9 (Invitrogen) were added to samples and incubated on a HulaMixer™ sample mixer at 4°C overnight. The following day the beads were briefly centrifuged, separated by a magnet from the supernatant, washed and resuspended in PBS.

Transfer experiments (Protein)—HeLa cells were seeded in 96-well culture plates (seeding density 5×10^3 cells/well). EVs and protein fractions were added to the cells 4 h after seeding. Nluc expression in medium and cells was analyzed at different times (0/24/48/72 h). To remove any non-internalized particles the cells were treated with 0.25% trypsin-EDTA (Thermofisher) for 30 min at 37°C and then washed in PBS twice (two centrifugations at 2,000 × g for 5 min each), resuspended in 50 μL PBS and seeded into 96-well white bottom Greiner Bio-one plates.

Transfer experiments (RNA)—HeLa cells were seeded in 96-well culture plates (seeding density 5×10^3 cells/well) and cycloheximide (1 μg/mL) was added 30 min before addition of EVs. Nano luciferase expression in media and cells (T0 and T24) was analyzed at the same time.

RNA data generation—RNA was extracted from concentrated EVs using the miRNeasy Mini Kit (Qiagen), according to the manufacturer's protocol.

cDNA synthesis and qPCR—cDNA was synthesized from extracted RNA using the RT Sensiscript kit (Qiagen) with Oligo dT Primer (Invitrogen) and RNase Inhibitor (Applied Biosystems). Samples were incubated at 37°C for 1 h. Primers were designed as follows for H2B: 5′ flanking primers: forward primer; 5′−3′, agcaagggcgaggaggtcatcaaag, reverse primer; 5′−3′, cggtgccggagctgccgctgccggt, 3′ Flanking primers: forward primer; 5′−3′, catcatcccgtatgaaggtctgagc, reverse primer; 5′−3′, ttacttagcgctggtgtacttggtg. Primers for HPRT1: forward primer; 5′−3′, tgacactggcaaaacaatg, reverse primer; 5′−3′, ggtccttttcaccagcaaa. qPCR was performed using PowerUp™ SYBR™ Green Master Mix (Applied Biosystems).

Confocal-imaging—COX-EVs from HEK293T cells were added to HeLa palmTdTom cells and then incubated for 72 h in 96-well culture plates. Cells were trypsinised (0.25%, 30 min @ 37°C) and plated onto Millicell EZ SLIDE 4-well glass (seeding density 5×10^3 cells) overnight. The images were acquired using a Zeiss LSM 800 Airyscan microscope (Oberkochen, Germany) using airyscan mode. 63x Objective with 1.4 NA lens was used for image acquisition. Airyscan images were processed using Huygens software (Scientific Volume Imaging B.V, Hilversum, The Netherlands). Microscopy Core of the Program in Membrane Biology.

Image analysis—Images were analyzed using FIJI (Schindelin et al., 2012). Regions of interest within cell boundary were measured for fluorescence intensity whereby the signal measured in control samples were designated as background. EV-exposed cells were then quantified with threshold adapted from control images. A line was graphed through points of interest and fluorescence intensity was plotted using FIJI.

Immunocytochemistry—Cells were rinsed in PBS and fixed in 4% paraformaldehyde (PFA; Electron Microscopy Sciences) for 10 min at RT. Cells were blocked and permeabilized in 3% Bovine Serum Albumin (BSA) in PBS with),1% Tween-20. Samples were incubated with primary antibody (TOM20 D8T4N, Rabbit mAb, 42406, Cell Signalling) overnight at 4°C. Samples were washed with PBS and secondary antibody

(Alexa Fluor 647, A31573, Donkey anti rabbit, Invitrogen) was incubated at RT for 1 h. Samples were mounted in Vectashield® Antifade (Vector Laboratories).

Cell fractionation—Fractionation of recipient cells was performed using the 'Cell Fractionation Kit – High throughput' (ab109718, Abcam, Cambridge, UK). Recipient cells were trypsinized for 30 min (0.25% trypsin). This method was performed in wells of a 96-well plate as per manufacturer guidelines (Lian et al., 2020). Bioluminescent signal was measured in samples following fractionation.

Re-release of free and EV-encapsulated Protein—EVs from HEK293T cells were added to HeLa cells seeded in 96-well culture plates (seeding density 5×10^3 cells/well) and incubated for 24/48 h. The recipient cells were trypsinized for 30 min with 0.25% trypsin in PBS and washed twice in PBS (two centrifugations at 2,000 × g for 5 min each). Cells were re-seeded in 96-well culture plates and after 48 h media (an aliquot) and cells were analyzed after incubation with CD63/CD9 beads (see above).

QUANTIFICATION AND STATISTICAL ANALYSIS

Data were analyzed using GraphPad Prism 6, version 6.04 (GraphPad Software Inc., La Jolla, CA).

Supplementary Material

Refer to Web version on PubMed Central for supplementary material.

ACKNOWLEDGMENTS

We thank Prof. Nagai (Osaka University) for sharing his reporter constructs with us. Imaging was performed in the Microscopy Core of the Program in Membrane Biology, which is partially supported by Centre for the Study of Inflammatory Bowel Disease grant DK043351 and Boston Area Diabetes Endocrinology Research Center (BADERC) award DK057521. The Zeiss confocal system is supported by NIH grant 1S10OD021577-01. Funding to the Breakefield laboratory was through NIH NCI CA069246 and CA232103. S.U. acknowledges financial support from Associazione Italiana per la Ricerca sul Cancro (grant IG 20210) (to S. Giordano).

REFERENCES

Ali SA, Teow SY, Omar TC, Khoo ASB, Choon TS, and Yusoff NM (2016). A cell internalizing antibody targeting capsid protein (p24) inhibits the replication of HIV-1 in T cells lines and PBMCS: a proof of concept study. PLoS One 11, e0145986. 10.1371/journal.pone.0145986. [PubMed: 26741963]

Antes TJ, Middleton RC, Luther KM, Ijichi T, Peck KA, Liu WJ, and Marbán E (2018). Targeting extracellular vesicles to injured tissue using membrane cloaking and surface display. J. Nanobiotechnol. 16, 1–15. 10.1186/s12951-018-0388-4.

Benedikter BJ, Benedikter BJ, Bouwman FG, Vajen T, Heinzmann AC, Grauls G, Mariman EC, and Stassen FR (2017). Ultrafiltration combined with size exclusion chromatography efficiently isolates extracellular vesicles from cell culture media for compositional and functional studies. Sci. Rep. 7, 1–13. 10.1038/s41598-017-15717-7. [PubMed: 28127051]

Christianson HC, Christianson HC, Svensson KJ, Van Kuppevelt TH, Li JP, and Belting M (2013). Cancer cell exosomes depend on cell-surface heparan sulfate proteoglycans for their internalization and functional activity. Proc. Natl. Acad. Sci. U S A. 110, 17380–17385. 10.1073/pnas.1304266110. [PubMed: 24101524]

Costa Verdera H, Verdera HC, Gitz-Francois JJ, Schiffelers RM, and Vader P (2017). Cellular uptake of extracellular vesicles is mediated by clathrin-independent endocytosis and macropinocytosis. J. Control. Release 266, 100–108. 10.1016/j.jconrel.2017.09.019. [PubMed: 28919558]

Cullen PJ, and Steinberg F (2018). To degrade or not to degrade: mechanisms and significance of endocytic recycling. Nat. Rev. Mol. Cell Biol. 19, 679–696. 10.1038/s41580-018-0053-7. [PubMed: 30194414]

Geoffroy C, Gaillard JL, Alouf JE, and Berche P (1987). Purification, characterization, and toxicity of the sulfhydryl-activated hemolysin listeriolysin O from Listeria monocytogenes. Infect. Immun. 55, 1641–1646. [PubMed: 3110067]

Grove J, and Marsh M (2011). The cell biology of receptor-mediated virus entry. J. Cell Biol. 195, 1071–1082. 10.1083/jcb.201108131. [PubMed: 22123832]

Guerreiro EM, Guerreiro EM, Vestad B, Steffensen LA, Aass HCD, Saeed M, Øvstebø R, and Søland TM (2018). Efficient extracellular vesicle isolation by combining cell media modifications, ultrafiltration, and size-exclusion chromatography. PLoS One 13, e0204276. 10.1371/journal.pone.0204276. [PubMed: 30260987]

Gurunathan S, Gurunathan S, Kang MH, Jeyaraj M, Qasim M, and Kim JH (2019). Review of the isolation, characterization, biological function, and multifarious therapeutic approaches of exosomes. Cells 8, 307. 10.3390/cells8040307.

Hall MP, Hall MP, Unch J, Binkowski BF, Valley MP, Butler BL, Wood MG, and Wood KV (2012). Engineered luciferase reporter from a deep sea shrimp utilizing a novel imidazopyrazinone substrate. ACS Chem. Biol. 7, 1848–1857. 10.1021/cb3002478. [PubMed: 22894855]

Haney MJ, Haney MJ, Zhao Y, Harrison EB, Mahajan V, Ahmed S, He Z, and Batrakova EV (2013). Specific transfection of inflamed brain by macrophages: a new therapeutic strategy for neurodegenerative diseases. PLoS One 8, e61852. 10.1371/journal.pone.0061852. [PubMed: 23620794]

Harding C, Heuser J, and Stahl P (1983). Receptor-mediated endocytosis of transferrin and recycling of the transferrin receptor in rat reticulocytes. J. Cell Biol. 97, 329–339. 10.1083/jcb.97.2.329. [PubMed: 6309857]

Hessvik NP, Phuyal S, Brech A, Sandvig K, and Llorente A (2012). Profiling of microRNAs in exosomes released from PC-3 prostate cancer cells. Biochim. Biophys. Acta Gene Regul. Mech. 1819, 1154–1163. 10.1016/j.bbagrm.2012.08.016.

Hopkins CR (1983). Intracellular routing of transferrin and transferrin receptors in epidermoid carcinoma A431 cells. Cell 35, 321–330. 10.1016/0092-8674(83)90235-0. [PubMed: 6313227]

Hopkins CR, and Trowbridge IS (1983). Internalization and processing of transferrin and the transferrin receptor in human carcinoma A431 cells. J. Cell Biol. 97, 508–521. 10.1083/jcb.97.2.508. [PubMed: 6309862]

Hsiao J-C, Hsiao JC, Chu LW, Lo YT, Lee SP, Chen TJ, Huang CY, and Chang W (2015). Intracellular transport of vaccinia virus in HeLa cells requires WASH-VPEF/FAM21-Retromer complexes and recycling molecules Rab11 and Rab22. J. Virol. 89, 8365–8382. 10.1128/jvi.00209-15. [PubMed: 26041286]

Hung ME, and Leonard JN (2016). A platform for actively loading cargo RNA to elucidate limiting steps in EV-mediated delivery. J. Extracell. Vesicles 5, 31027. 10.3402/jev.v5.31027. [PubMed: 27189348]

Hurwitz SN, and Meckes DG (2019). Extracellular vesicle integrins distinguish unique cancers. Proteomes 7, 14. 10.3390/proteomes7020014. [PubMed: 30979041]

Iversen TG, Skotland T, and Sandvig K (2011). Endocytosis and intracellular transport of nanoparticles: present knowledge and need for future studies. Nano Today 6, 176–185. 10.1016/j.nantod.2011.02.003.

Joshi BS, Joshi BS, de Beer MA, Giepmans BN, and Zuhorn IS (2020). Endocytosis of extracellular vesicles and release of their cargo from endosomes. ACS Nano 14, 9. 10.1021/acsnano.9b10033.

Lai CP, Mardini O, Ericsson M, Prabhakar S, Maguire CA, Chen JW, and Breakefield XO (2014). Dynamic biodistribution of extracellular vesicles in vivo using a multimodal imaging reporter. ACS Nano 8, 483–494. 10.1021/nn404945r. [PubMed: 24383518]

Lai CP, Lai CP, Kim EY, Badr CE, Weissleder R, Mempel TR, Tannous BA, and Breakefield XO (2015). Visualization and tracking of tumour extracellular vesicle delivery and RNA translation using multiplexed reporters. Nat. Commun. 6, 1–12. 10.1038/ncomms8029.

Lian J, Zou Y, Huang L, Cheng H, Huang K, Zeng J, and Chen L (2020). Hepatitis B virus upregulates cellular inhibitor of apoptosis protein 2 expression via the PI3K/AKT/NF–kB signaling pathway in liver cancer. Oncol. Lett. 19, 2043–2052. 10.3892/ol.2020.11267. [PubMed: 32194701]

Linares R, Tan S, Gounou C, Arraud N, and Brisson AR (2015). High-speed centrifugation induces aggregation of extracellular vesicles. J. Extracell. Vesicles 4, 29509. 10.3402/jev.v4.29509. [PubMed: 26700615]

Ludwig N, Razzo BM, Yerneni SS, and Whiteside TL (2019). Optimization of cell culture conditions for exosome isolation using mini-size exclusion chromatography (mini-SEC). Exp. Cell Res. 378, 149–157. 10.1016/j.yexcr.2019.03.014. [PubMed: 30857972]

Mainou BA, and Dermody TS (2012). Transport to late endosomes is required for efficient reovirus infection. J. Virol. 86, 8346–8358. 10.1128/jvi.00100-12. [PubMed: 22674975]

Marsh EW, Leopold PL, Jones NL, and Maxfield FR (1995). Oligomerized transferrin receptors are selectively retained by a lumenal sorting signal in a long-lived endocytic recycling compartment. J. Cell Biol. 129, 1509–1522. 10.1083/jcb.129.6.1509. [PubMed: 7790351]

Mathieu M, Mathieu M, Martin-Jaular L, Lavieu G, and Théry C (2019). Specificities of secretion and uptake of exosomes and other extracellular vesicles for cell-to-cell communication. Nat. Cell Biol. 21, 9–17. 10.1038/s41556-018-0250-9. [PubMed: 30602770]

McCabe JB, and Berthiaume LG (1999). Functional roles for fatty acylated amino-terminal domains in subcellular localization. Mol. Biol. Cell 10, 3771–3786. 10.1091/mbc.10.11.3771. [PubMed: 10564270]

Momose F, Momose F, Sekimoto T, Ohkura T, Jo S, Kawaguchi A, Nagata K, and Morikawa Y (2011). Apical transport of influenza A virus ribonucleoprotein requires Rab11-positive recycling endosome. PLoS One 6, 21123. 10.1371/journal.pone.0021123.

Mulcahy LA, Pink RC, and Carter DRF (2014). Routes and mechanisms of extracellular vesicle uptake. J. Extracell. Vesicles 32, 24641. 10.3402/jev.v3.24641.

O'Brien K, O'Brien K, Breyne K, Ughetto S, Laurent LC, and Breakefield XO (2020). RNA delivery by extracellular vesicles in mammalian cells and its applications. Nat. Rev. Mol. Cell Biol. 21, 585–606. 10.1038/s41580-020-0251-y. [PubMed: 32457507]

Oksvold MP, Neurauter A, and Pedersen KW (2015). Magnetic bead-based isolation of exosomes. Methods Mol. Biol 10.1007/978-1-4939-1538-5_27.

Pan BT, and Johnstone RM (1983). Fate of the transferrin receptor during maturation of sheep reticulocytes in vitro: selective externalization of the receptor'. Cell 33, 967–978. 10.1016/0092-8674(83)90040-5. [PubMed: 6307529]

Pedersen KW, Pedersen KW, Kierulf B, Oksvold MP, Li M, Vlassov AV, Roos N, and Neurauter A (2013). Isolation and characterization of exosomes using magnetic beads. BioProbes 71, 10–13.

Polanco JC, Polanco JC, Hand GR, Briner A, Li C, and Gö tz J (2021). Exosomes induce endolysosomal permeabilization as a gateway by which exosomal tau seeds escape into the cytosol. Acta Neuropathol. 141, 235–256. 10.1007/s00401-020-02254-3. [PubMed: 33417012]

Qin Y, Jiang X, Yang Q, Zhao J, Zhou Q, and Zhou Y (2021). The functions, methods, and mobility of mitochondrial transfer between cells. Front Oncol. 11. 10.3389/FONC.2021.672781.

Raposo G, Nijman HW, Stoorvogel W, Liejendekker R, Harding CV, Melief CJ, and Geuze HJ (1996). B lymphocytes secrete antigen-presenting vesicles. J. Exp. Med. 183, 1161–1172. 10.1084/jem.183.3.1161. [PubMed: 8642258]

Ratajczak J, Ratajczak J, Miekus K, Kucia M, Zhang J, Reca R, Dvorak P, and Ratajczak MZ (2006). Embryonic stem cell-derived microvesicles reprogram hematopoietic progenitors: evidence for horizontal transfer of mRNA and protein delivery. Leukemia 20, 847–856. 10.1038/sj.leu.2404132. [PubMed: 16453000]

Rowe RK, Suszko JW, and Pekosz A (2008). Roles for the recycling endosome, Rab8, and Rab11 in hantavirus release from epithelial cells. Virology 382, 239–249. 10.1016/j.virol.2008.09.021. [PubMed: 18951604]

Rustom A, Rustom A, Saffrich R, Markovic I, Walther P, and Gerdes HH (2004). Nanotubular highways for intercellular organelle transport. Science 303, 1007–1010. 10.1126/science.1093133. [PubMed: 14963329]

Schindelin J, Schindelin J, Arganda-Carreras I, Frise E, Kaynig V, Long-air M, Pietzsch T, and Cardona A (2012). Fiji: an open-source platform for biological-image analysis. Nat. Methods 9, 676–682. 10.1038/nmeth.2019. [PubMed: 22743772]

Schnell JR, and Chou JJ (2008). Structure and mechanism of the M2 proton channel of influenza A virus. Nature 451, 591–595. 10.1038/nature06531. [PubMed: 18235503]

Selby LI, Cortez-Jugo CM, Such GK, and Johnston AP (2017). Nanoescapology: progress toward understanding the endosomal escape of polymeric nanoparticles. Wiley Interdiscip. Rev. Nanomed. Nanobiotechnol. 9, e1452. 10.1002/wnan.1452.

Sena-Esteves M, Sena-Esteves M, Tebbets JC, Steffens S, Crombleholme T, and Flake AW (2004). Optimized large-scale production of high titer lentivirus vector pseudotypes. J. Virol. Methods 122, 131–139. 10.1016/j.jviromet.2004.08.017. [PubMed: 15542136]

Shukla D, Shukla D, Liu J, Blaiklock P, Shworak NW, Bai X, Esko JD, and Spear PG (1999). A novel role for 3-O-sulfated heparan sulfate in herpes simplex virus 1 entry. Cell 99, 13–22. 10.1016/S0092-8674(00)80058-6. [PubMed: 10520990]

Skog J, Skog J, Wurdinger T, Van Rijn S, Meijer DH, Gainche L, Curry WT, and Breakefield XO (2008). Glioblastoma microvesicles transport RNA and proteins that promote tumour growth and provide diagnostic biomarkers. Nat. Cell Biol. 10, 1470–1476. 10.1038/ncb1800. [PubMed: 19011622]

Suzuki K, Suzuki K, Kimura T, Shinoda H, Bai G, Daniels MJ, Arai Y, and Nagai T (2016). Five colour variants of bright luminescent protein for real-time multicolour bioimaging. Nat. Commun. 7, 1–10. 10.1038/ncomms13718.

Svensson KJ, Svensson KJ, Christianson HC, Wittrup A, Bourseau-Guilmain E, Lindqvist E, Svensson LM, and Belting M (2013). Exosome uptake depends on ERK1/2-heat shock protein 27 signaling and lipid raft-mediated endocytosis negatively regulated by caveolin-1. J. Biol. Chem. 288, 17713–17724. 10.1074/jbc.M112.445403. [PubMed: 23653359]

Théry C, Théry C, Witwer KW, Aikawa E, Alcaraz MJ, Anderson JD, Andriantsitohaina R, and Jovanovic-Talisman T (2018). Minimal information for studies of extracellular vesicles 2018 (MISEV2018): a position statement of the International Society for Extracellular Vesicles and update of the MISEV2014 guidelines. J. Extracell. Vesicles 7, 1535750. 10.1080/20013078.2018.1535750. [PubMed: 30637094]

Tian T, Wang Y, Wang H, Zhu Z, and Xiao Z (2010). Visualizing of the cellular uptake and intracellular trafficking of exosomes by live-cell microscopy. J. Cell Biochem. 111, 488–496. 10.1002/jcb.22733. [PubMed: 20533300]

Tkach M, Tkach M, Kowal J, Zucchetti AE, Enserink L, Jouve M, Lankar D, and Théry C (2017). Qualitative differences in T-cell activation by dendritic cell-derived extracellular vesicle subtypes. EMBO J. 36, 3012–3028. 10.15252/embj.201696003. [PubMed: 28923825]

Tweten RK (2005). Cholesterol-dependent cytolysins, a family of versatile pore-forming toxins. Infect. Immun. 73, 6199–6209. 10.1128/IAI.73.10.6199-6209.2005. [PubMed: 16177291]

Utley TJ, Utley TJ, Ducharme NA, Varthakavi V, Shepherd BE, Santangelo PJ, Lindquist ME, and Crowe JE (2008). Respiratory syncytial virus uses a Vps4-independent budding mechanism controlled by Rab11-FIP2. Proc. Natl. Acad. Sci. U S A. 105, 10209–10214. 10.1073/pnas.0712144105. [PubMed: 18621683]

Valadi H, Valadi H, Ekström K, Bossios A, Sjöstrand M, Lee JJ, and Lötvall JO (2007). Exosome-mediated transfer of mRNAs and microRNAs is a novel mechanism of genetic exchange between cells. Nat. Cell Biol. 9, 654–659. 10.1038/ncb1596. [PubMed: 17486113]

van Ijzendoorn SCD (2006). Recycling endosomes. J. Cell Sci. 35, 117–122. 10.1242/jcs.02948.

Wang X, Qiao D, Chen L, Xu M, Chen S, Huang L, and Fu L (2019). Chemotherapeutic drugs stimulate the release and recycling of extracellular vesicles to assist cancer cells in developing an urgent chemoresistance. Mol. Cancer 18, 1–18. 10.1186/s12943-019-1114-z. [PubMed: 30609930]

Wei Z, Batagov AO, Schinelli S, Wang J, Wang Y, El Fatimy R, and Krichevsky AM (2017). Coding and noncoding landscape of extracellular RNA released by human glioma stem cells. Nat. Commun. 8, 1–15. 10.1038/s41467-017-01196-x. [PubMed: 28232747]

Wiklander OPB, Wiklander OP, Brennan MÁ, Lötvall J, Breakefield XO, and El Andaloussi S (2019). Advances in therapeutic applications of extracellular vesicles. Sci. Transl. Med 11, eaav8521. 10.1126/scitranslmed.aav8521. [PubMed: 31092696]

Xiao Z, Xiao Z, Shangguan D, Cao Z, Fang X, and Tan W (2008). Cell-specific internalization study of an aptamer from whole cell selection. Chem. Eur. J. 14, 1769–1775. 10.1002/chem.200701330. [PubMed: 18092308]

Zila V, Zila V, Difato F, Klimova L, Huerfano S, and Forstova J (2014). Involvement of microtubular network and its motors in productive endocytic trafficking of mouse polyomavirus. PLoS One 9, e96922. 10.1371/journal.pone.0096922. [PubMed: 24810588]

Highlights

- Size-exclusion chromatography isolates a highly purified population of vesicles
- Extracellular vesicles (EVs) can be internalized in a "non-functional" manner
- Functional release of EV cargo into the cytosol is inefficient in tested cells
- EVs can be re-released intact from recipient cells

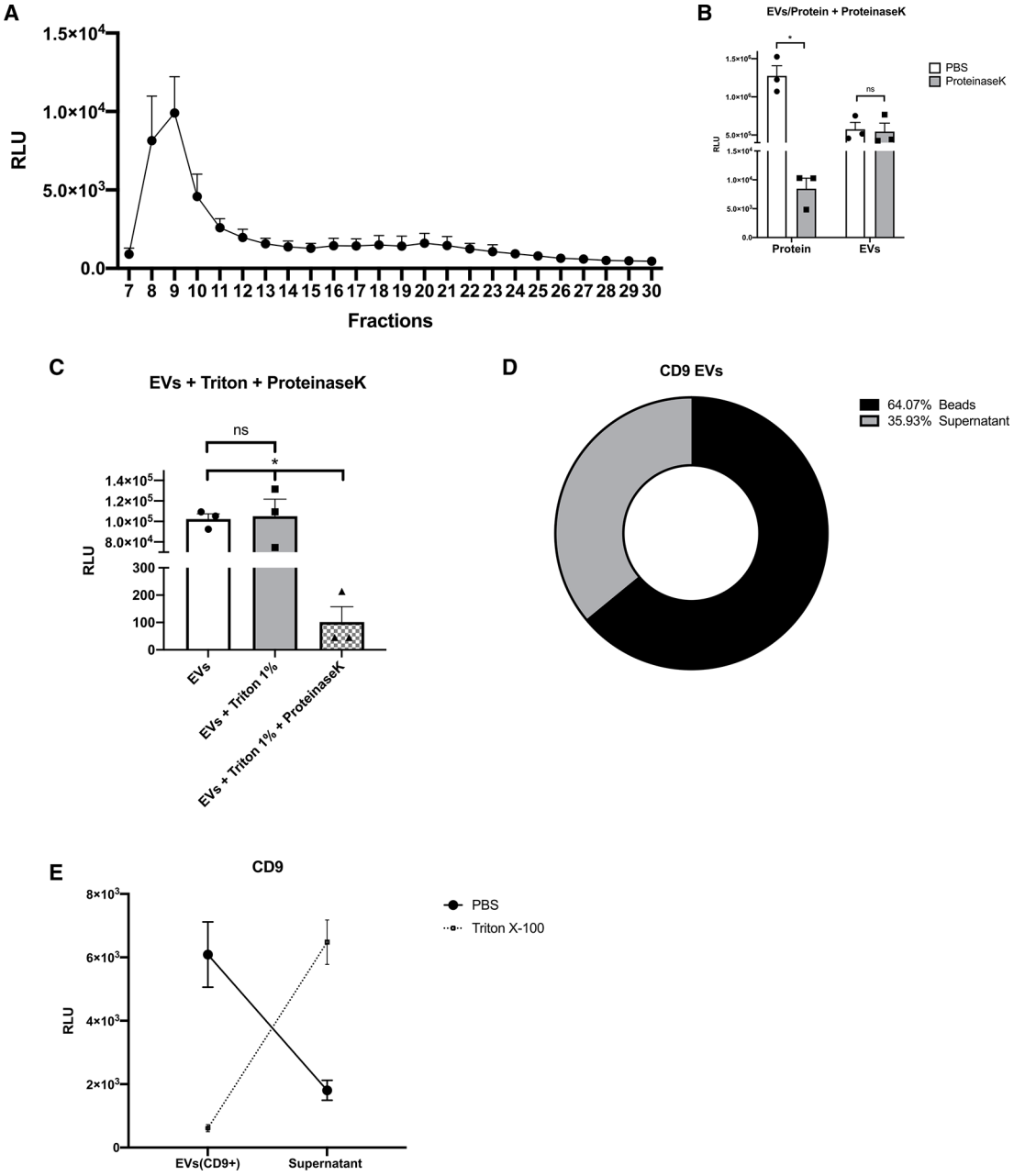

Figure 1. Isolation and characterization of EVs

(A) Full bioluminescence profile analysis of EVs (fractions 7–11) that were isolated, concentrated, and run through SEC to show the purity of the isolate analyzed by bioluminescence (n = 3, SEM).

(B) Treatment of isolated protein (fraction 19) and EVs (fractions 7–11) from initial SEC resolution (Figure S1A) with Proteinase K to demonstrate protection of encapsulated protein in EVs (n = 3, SEM).

(C) Treatment of isolated EVs (7–11) with 1% Triton X-100 and then Proteinase K to show that it is possible to degrade the initially protected cargo when the membrane is permeabilized (n = 3, SEM).

(D) Incubation of isolated EVs with magnetic CD9 beads and subsequent pull-down and analysis to demonstrate the proportion of $CD9^+$ vesicles in whole isolate (n = 3, SEM).
(E) Incubation of vesicles with PBS or 1% Triton X-100 and subsequent incubation with CD9 beads to demonstrate the association of the protein with $CD9^+$ vesicles before disruption of the membrane and after disruption, where the signal is not pulled down with $CD9^+$ beads (n = 3, SEM).
ns, no significance; *$p < 0.05$.

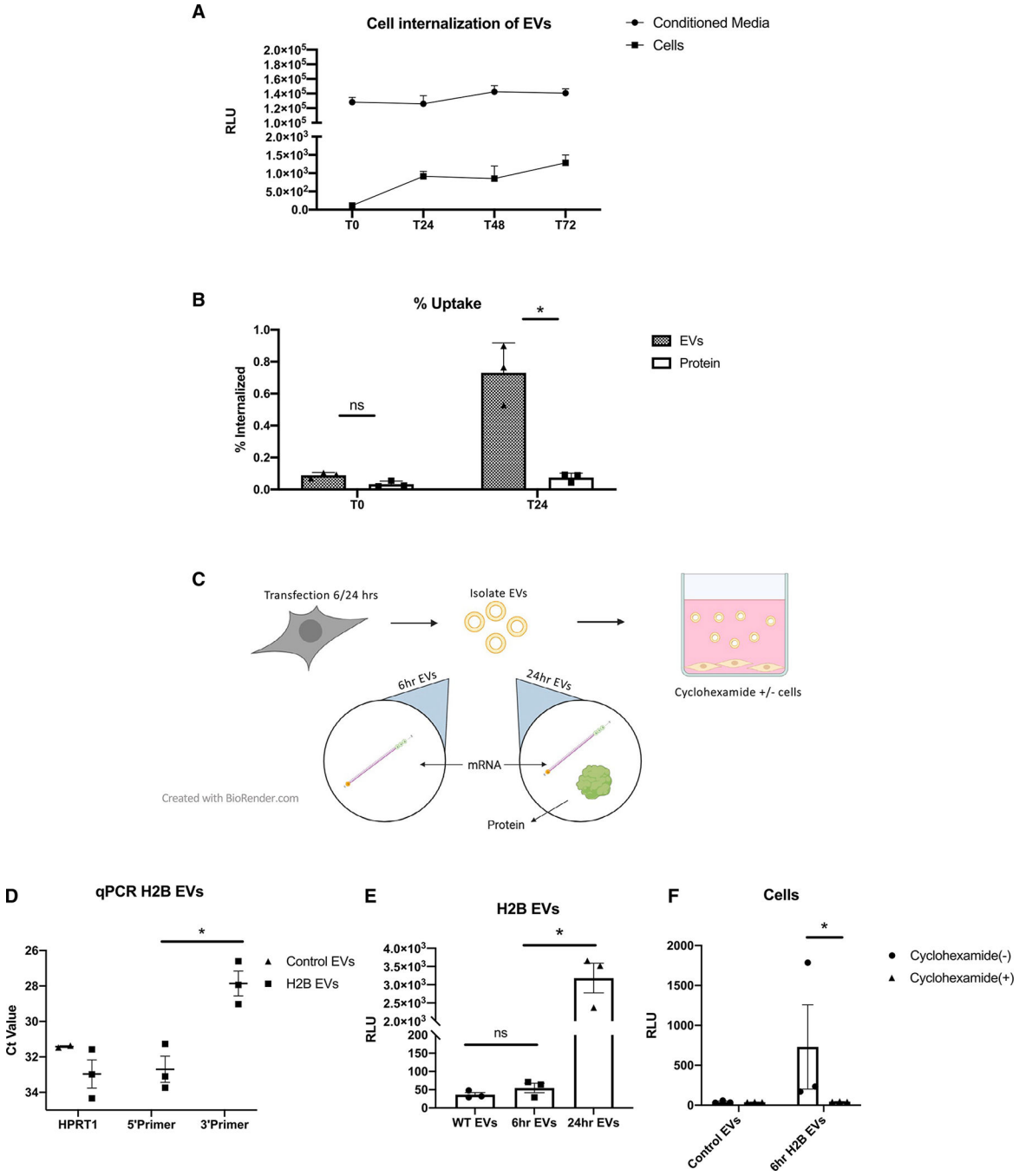

Figure 2. Internalization of EV cargo and translation of EV mRNA

(A) Analysis of internalization of HEK EVs into recipient HeLa cells as analyzed at T0 and T24 by bioluminescence imaging (n = 3, SEM).

(B) Efficiency of internalization of EVs versus protein. The luminescent signal in the cells was divided by the total signal in the medium plus signal in the cell to estimate efficiency of uptake. Although the efficiencies were relatively low (<1%), EVs demonstrated greater efficiency over time compared with protein by 3- to 10-fold (n = 3, SEM).

(C) Schematic of the strategy to evaluate mRNA translation in recipient cells by harvesting EVs before (6 h) or after (24 h) detectable translation in donor cells.
(D) qRT-PCR analysis of RNA in isolated EVs with primers of HPRT mRNA and 5′ and −3′ prime ends of H2B mRNA. The lack of a data point relates to non-detection below a Ct (Cycle threshold) of 35 Ct (n = 3, SEM).
(E) Analysis of isolated EVs for the presence of the H2B protein by bioluminescence (n = 3, SEM).
(F) Transfer of isolated 6-h EVs to recipient cells treated with cycloheximide versus control to evaluate translation of mRNA to detectable levels of the protein by bioluminescence of cells (n = 3, SEM).
*$p < 0.05$.

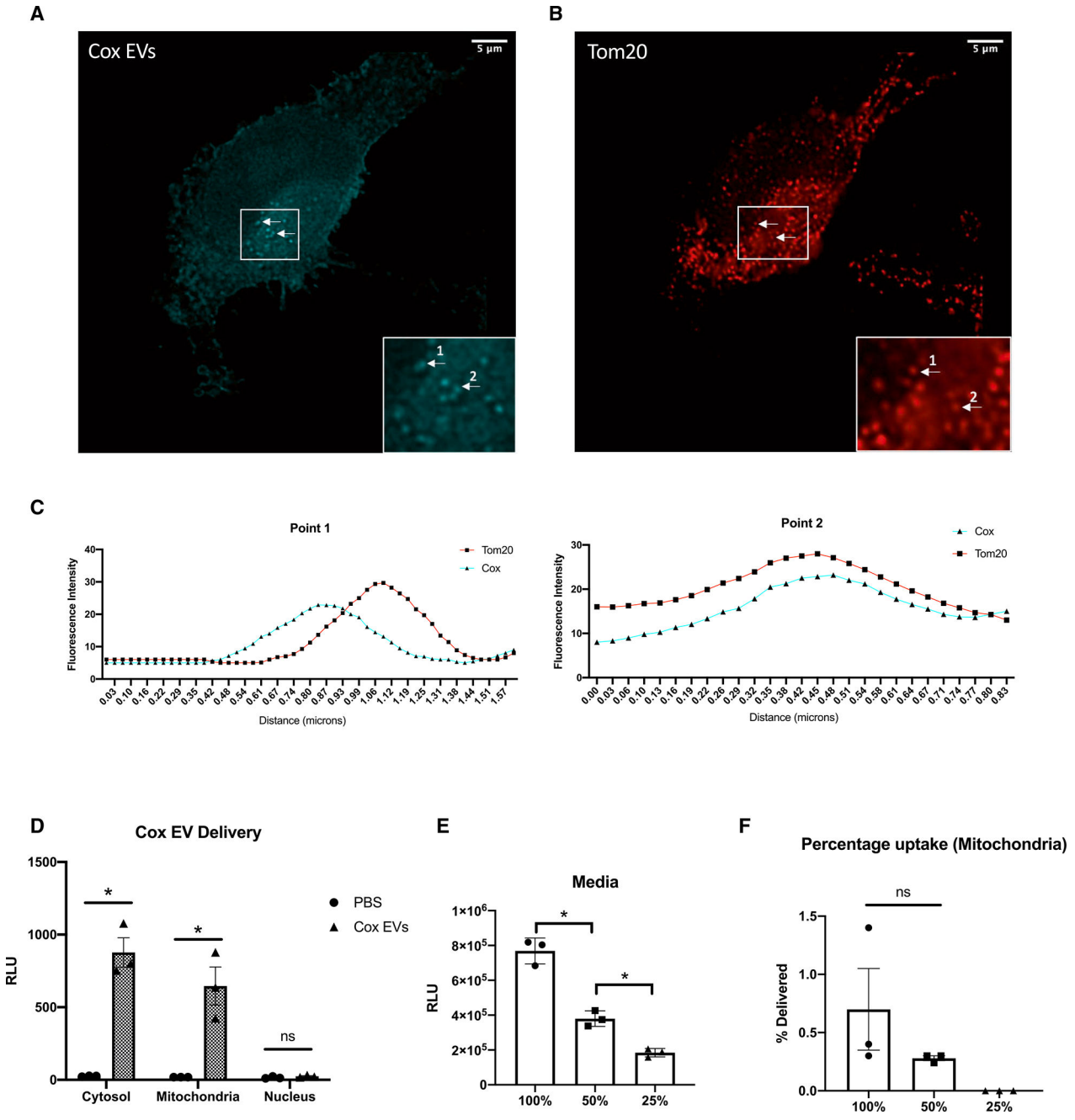

Figure 3. Functional delivery of bioluminescent Cox protein

(A and B) Representative images of recipient HeLa cells incubated with Cox EVs and stained with the mitochondrial marker Tom20 (n = 3, scale bars, 5 µm).

(C) Fluorescence intensity profile of selected regions, demonstrating co-localization of Cox protein with mitochondria, with the fluorescent intensity profile showing little to no colocalization of Cox protein and membrane signal.

(D) Cell fractions analyzed by luminescence detection of the Cox protein in cytosol and mitochondrial fractions, with no detection of signal in the nuclear fraction (n = 3, SEM). </p/>(E and F) A sequential dilution of isolated EVs (100%, 50%, and 25%) was added to

recipient HeLa cells for 72 h; they were then fractionated to determine the percentage of uptake into mitochondria (signal in mitochondrial fraction/total signal in media × 100) (n = 3, SEM). </p/>*p < 0.05.

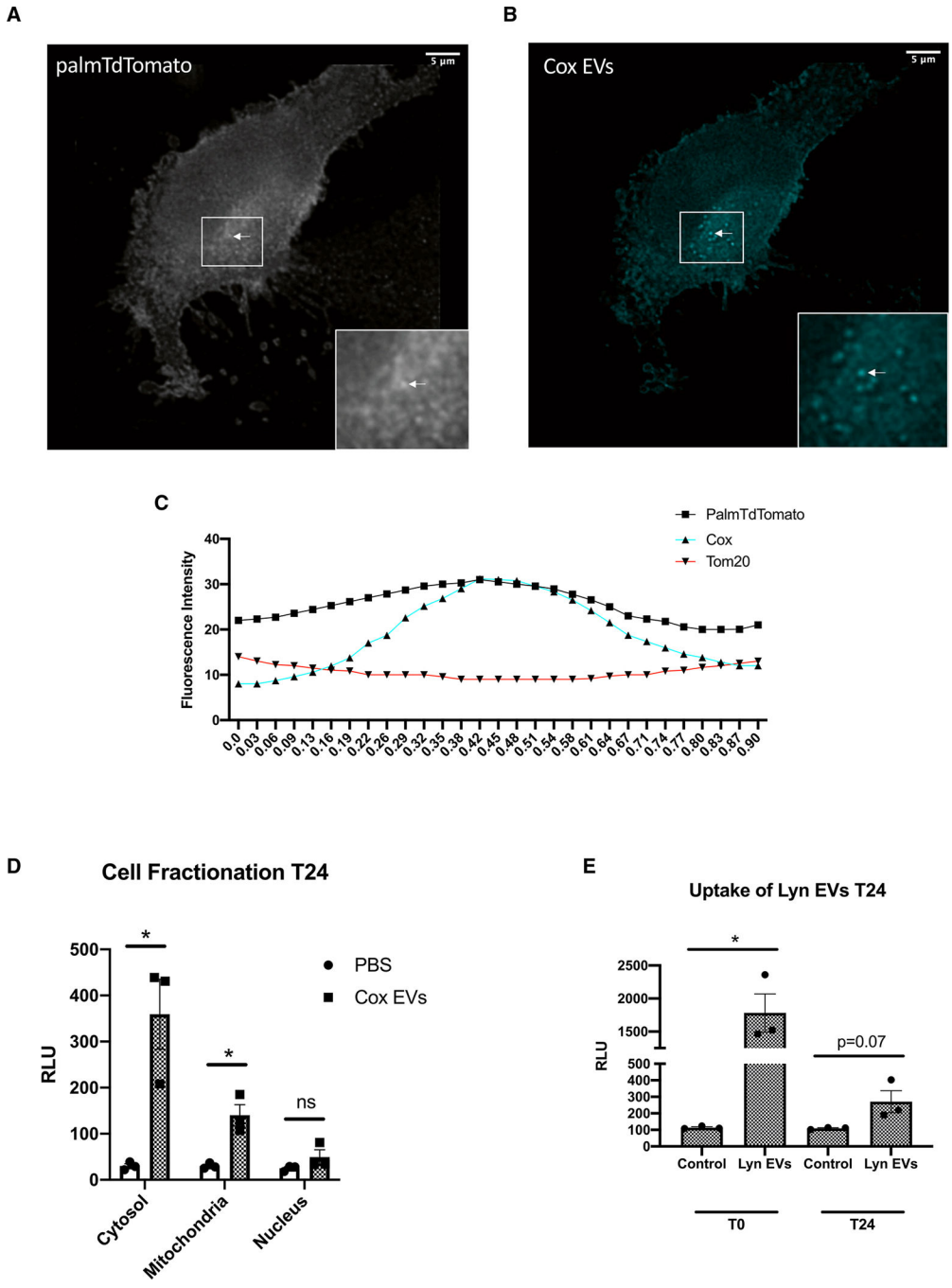

Figure 4. Retention of EV cargo in a non-functional manner

(A and B) Images of cells exposed to EVs and subsequently re-seeded in EV-free medium for 24 h to show that the Cox signal localized with the palmTdTomato signal, showing retention of the signal in the endosomal compartment (n = 3; scale bars, 5 µm).

(C) Fluorescence intensity profile of palmTdTomato, Cox EVs, and Tom20.

(D) Luminescence analysis of fractionated recipient cells that had external EVs removed 24 h after exposure, showing strong signal in the cytosol (n = 3, SEM).

(E) Luminescence analysis of HeLa cells exposed to Lyn EVs with external signal removed, showing retention of signal in the recipient cells (n = 3, SEM).
*$p < 0.05$.

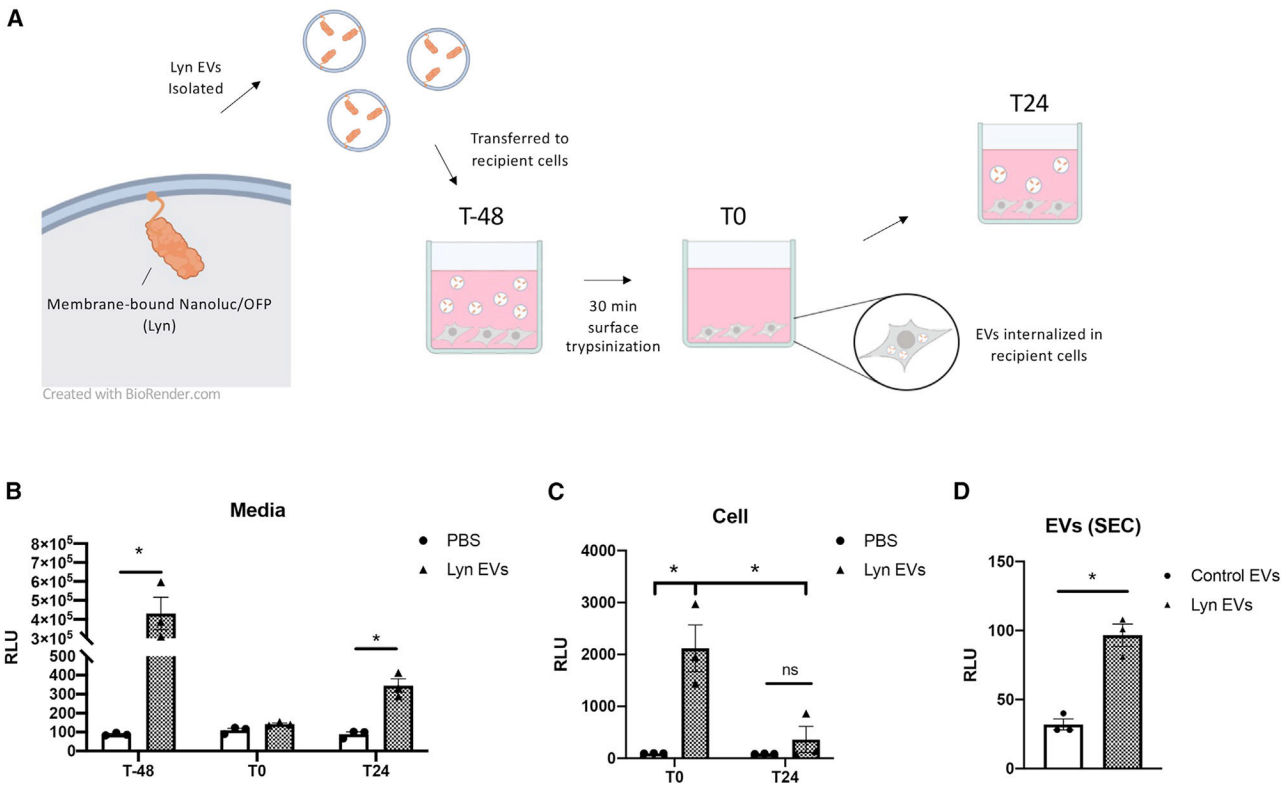

Figure 5. Re-release of membrane-bound protein

(A) Schematic overview of the experimental design, showing membrane-bound Nluc/GFP added to recipient HeLa cells and incubated for 48 h before 30-min trypsin (0.25%) treatment and washing, then re-seeding.

(B) Medium collected and analyzed over the course of the experiment, showing re-introduction of signal from the recipient cells 24 h after re-seeding (T24) (n = 3, SEM).

(C) Analysis of the EVs in the recipient cell 24 h after removal of external signal, showing a significant reduction in signal (n = 3, SEM).

(D) T24 Medium from a re-release experiment as shown was collected and run through SEC, where fractions 7–11 were collected and concentrated, and luminescent analysis showed a significant increase in Lyn EVs compared with non-treated EVs (n = 3, SEM).

*$p < 0.05$.

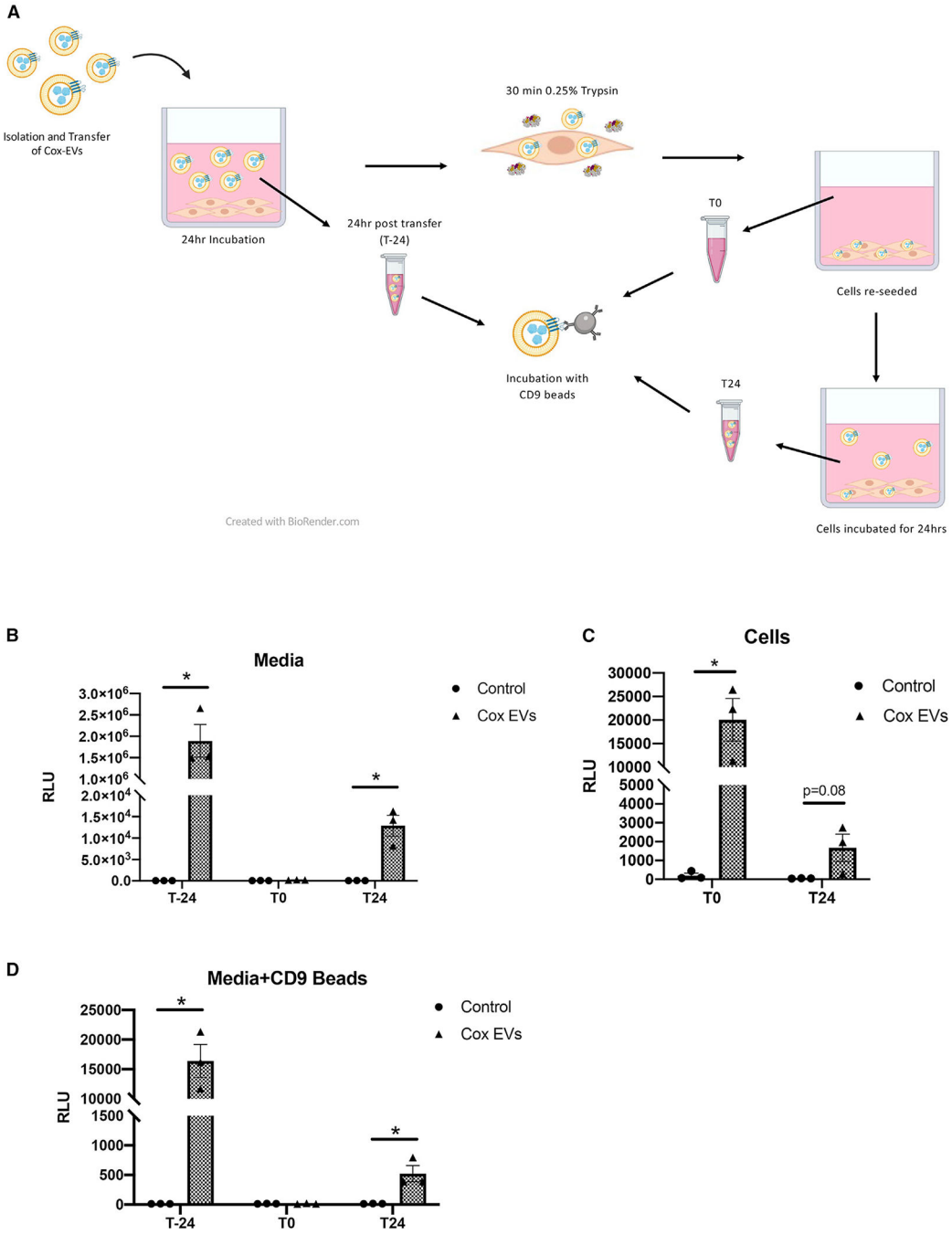

Figure 6. Re-release of EV cargo

(A) Schematic overview of the experimental design with final analysis by incubation with CD9-magnetic beads to confirm re-release of vesicles.

(B) Luminescence analysis of medium over the course of the experiment, showing significant re-introduction of signal into the medium derived from recipient cells (n = 3, SEM).

(C) Signal in cells showed a significant reduction over the 24 h after removal of external signal (n = 3, SEM).

(D) Incubation of the medium from (A), with CD9 magnetic beads showing localization of protein signal with $CD9^+$ vesicles after re-release (n = 3, SEM).
*$p < 0.05$.

KEY RESOURCES TABLE

REAGENT or RESOURCE	SOURCE	IDENTIFIER
Antibodies		
TOM20 Rabbit monoclonal Ab	Cell Signalling Technology	Cat# 42406; RRID:AB_2687663
Critical commercial assays		
Cell Fractionation Kit – High throughput	Abcam	ab109718
Nano-Glo® Luciferase	Promega	N1110
Human CD63 Isolation/Detection	Invitrogen	10606D
Exosome – Human CD9	Invitrogen	10614D
Experimental models: Cell lines		
Human embryonic kidney 293 (HEK293T)	ATCC	CRL-3216; RRID:CVCL_0063
HeLa cells	ATCC	CLS Cat# 300194/p772_HeLa; RRID:CVCL_0030